Estimation of the Damping Parameter Governing the VIV of Long Flexible Cylinders

Proceedings of the ASME 2015 34th International Conference on Ocean, Offshore and Arctic Engineering
OMAE2015
May 31-June 5, 2015, St. John's, Newfoundland, Canada

OMAE2015-41296

ESTIMATION OF THE DAMPING PARAMETER GOVERNING THE VIV OF LONG FLEXIBLE CYLINDERS

Zhibiao Rao[1]
Department of Mechanical Engineering
Massachusetts Institute of Technology
Cambridge, MA, USA

Prof. J. Kim Vandiver
Department of Mechanical Engineering
Massachusetts Institute of Technology
Cambridge, MA, USA

ABSTRACT

Much effort in the past half century has been made to explain the role of damping in the prediction of VIV. Scruton (1965), Griffin *et al.* (1975), Klamo, *et al.* (2005) and Govardhan & Williamson (2006) all made significant contributions. None fully characterized the role of damping in governing the response over the full range reduced velocities, which encompass the wake synchronized region. In 2012 Vandiver devised a way to do that with a new damping parameter c^*. His results were verified using 2D spring-mounted cylinders in uniform flow.

The primary objective of the research described in this paper is to find a c^*-like quantity for flexible cylinders, which is capable of organizing response data for flexible cylinders, which may have many modes, be exposed to sheared flows and possess spatially varying properties, such as the coverage of strakes and fairings. Data from a recent high mode VIV model test campaign conducted by SHELL Exploration and Production Company are used to illustrate the application of c^* to flexible cylinders. It is shown that, if one accounts for Reynolds number, the response of flexible cylinders with varying strake coverage in the SHELL Tests collapse onto a single curve.

INTRODUCTION

Since 1955, many authors have attempted to use the mass-damping parameter to explain the role of damping in the prediction of VIV. Griffin *et al.* (1975) attempted to collapse the VIV amplitude response of a wide variety of cylinders using the mass-damping parameter S_G. The "Griffin plot" had a lot of scatter (Sarpkaya, 2004). The scatter was the result of their attempt to include data from low mass ratio structures and data from structures with a variety of mode shapes. The most important limitation was they did not account for the role of Reynolds number.

Klamo *et al.* (2005) were the first to reveal that VIV peak response amplitude increased with Reynolds number in the sub-critical range.

Govardhan and Williamson (2006) conducted further experiments on spring-mounted cylinders with 1 and 2 degrees of freedom in uniform flow. Careful control of damping in their experiments enabled them to investigate the relationship between their damping parameter α and the peak-amplitude at a given Reynolds number. They successfully separated the effect of damping from that of Reynolds number and mass ratio.

As with all forms of mass-damping parameter, Govardhan and Williamson's α parameter only succeeds at characterizing the peak response of spring-mounted cylinders at resonance and performs worse for low mass ratio structures. Vandiver (2012) derived a new damping parameter c^* which overcame many of the limitations of mass-damping parameters mentioned above. This new damping parameter, c^*, is valid over the full lock-in range of reduced velocities. His results were verified using data from experiments with spring mounted cylinders in uniform flow.

The primary objective of the research described in this paper is to find a c^*-like quantity from flexible cylinders, which is capable of organizing response data for flexible cylinders, which may have many modes, be exposed to sheared flows and possess spatially varying properties, such as the coverage of strakes and fairings.

The largest challenges involve properly defining a damping coefficient for structurally non-uniform cylinders in non-uniform flow. For example, how does one characterize damping

[1] Corresponding Author, Zhibiao Rao, Email: zbrao@mit.edu

for a riser partially covered with helical strakes in a uniform flow?

EXPERIMENT DESCRIPTION

The experiments were conducted in 2011 by SHELL Exploration and Production in the Ocean Laboratory at MARINTEK, which is described in detail in Lie *et al.* (2012). Some results from these tests have already been published in a series of papers over the past few years, see Resvanis *et al.* (2012, 2014), Rao *et al*. (2012, 2013, 2014, 2015) and Rao (2015)

A 38 m long horizontal riser model was attached to the test rig via universal joints. Figure 1 shows the schematic of the test set-up in uniform flow. Clump weights were attached to the upper truss in a vertical pendulum configuration. The riser ends were are attached to the clump weights via universal joint and the force transducers.

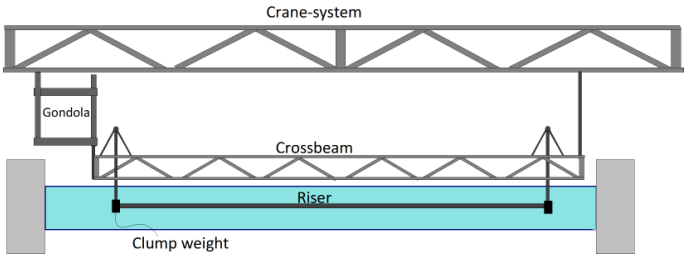

Figure 1 Schematic of the test set-up in uniform flow (MARINTEK, 2011).

Table 1 Pipe Model Properties for the SHELL Tests

Parameters	**Pipe**
Total length between pinned ends (m)	38.00
Outer diameter (Hydrodynamic Diameter) (mm)	80
Optical diameter (Strength Diameter) (mm)	27
Inner diameter (mm)	21
Bending stiffness, EI (Nm^2)	572.3
Young's modulus, E(N/m^2)	$3.46x10^{10}$
Mass/length in air (kg/m)	5.708
Weight in water (kg/m)	0.937
Mass ratio	1.14

The pipe was densely instrumented with Bragg fiber optic strain gauges at 30 equidistant locations. Additionally 22 bi-axial accelerometers were mounted inside the pipe to measure in-line and cross-flow accelerations. Tri-axial force transducers were installed at both ends. All transducers were sampled at a rate of 1200Hz. Pipe properties are listed in Table 1.

The pipe, partially covered with helical strakes, is the main focus of this paper. The triple start helical strakes were cast from polyurethane, and were delivered in sections 430mm long. Each complete section was made up of two half-shells attached to the 80mm pipe with plastic straps.

With 100% strake coverage the long flexible pipe exhibited no VIV. The strakes were then removed progressively from the center towards the ends so as to create a bare section in the middle. Figure 2 shows the schematic diagram of the pipe partially covered with helical strakes. Rao *et al.* (2014) used the vibration intensity technique to confirm that the bare sections of length L_{in} were in fact the power-in regions. Five straked configurations were tested in uniform flows: gap lengths tested were 5%, 15%, 25%, 52% and 100% of the total length. The Reynolds number spanned the range from 20,000 to 120,000.

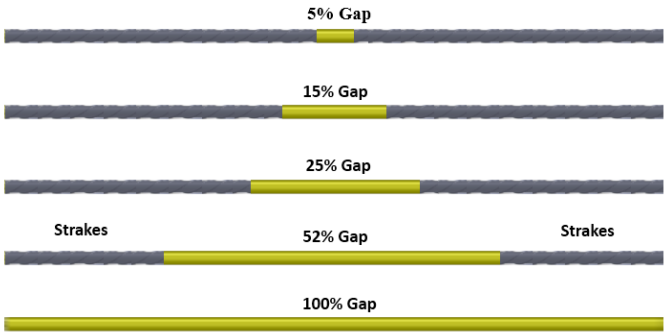

Figure 2 Schematic of the 80 mm diameter pipe with the five strake configurations.

THE C^* DAMPING PARAMETER FOR SPRING-MOUNTED, RIGID CYLINDERS

The damping parameter, c^*, was proposed by Vandiver (2012). It may be derived from the cross-flow equation of motion for a rigid cylinder. It is valid over the full range of reduced velocities for which the wake and cylinder motion are synchronized and is applicable to both high and low mass ratio cylinders. Vandiver's damping parameter for a rigid cylinder is defined as:

$$\boldsymbol{c^* = \frac{2c\omega}{\rho U^2}} \quad (1)$$

Where c is the damping constant per unit length of a rigid cylinder and has units of force per unit length per unit cylinder velocity. ω is the response frequency which does not have to coincide with the natural frequency, ρ is the fluid density and U is the flow speed.

Equation (1) is based on the assumption that any steady-state, periodic, VIV exciting force may be decomposed into a Fourier series. Thus c^* is valid at any steady state excitation frequency. The observed dimensionless response amplitude A^* need not be observed at resonance.

Govardan and Williamson (2006) showed that the effect of Reynolds number could be separated from that of damping. In Vandiver (2012) the G&W data was recast in terms of c^*. Figure 3 shows that data taken at several different Reynolds numbers collapse onto a single curve, after the Reynolds number dependence is removed from A^*. The plot shows the modified amplitude $A^*_{max}/f(Re)$ versus $log(c^*)$.

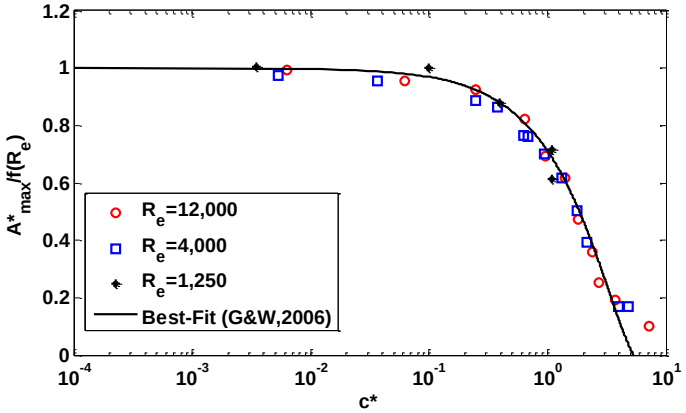

Figure 3 $A^*_{max}/f(Re)$ versus $log(c^*)$ for $Re = 1250 (m^* = 15.3)$, $Re = 4000 (m^* = 10.9)$ and $Re = 12000 (m^* = 10.3)$. The solid line represents the best-fit curve in Govardhan and Williamson (2006). This figure is based on the data shown in Fig.14, Govardhan and Williamson (2006).

The best-fit curve in Fig.3 represents the relationships between the modified peak-amplitude $A^*_{max}/f(Re)$ and damping parameter c^* which is written as

$$\boldsymbol{A^*_{max}/f(Re) = \left(1 - 0.31c^* + 0.023c^{*2}\right)} \quad (2)$$

Where A^*_{max} is the dimensionless peak amplitude, $f(Re) = log(0.41Re^{0.36})$ and Re is the Reynolds number.

DEFINITION OF THE EQUIVALENT DAMPING PARAMETER c^*_{eq} AND AMPLITUDE A^*_{eq} FOR FLEXIBLE CYLINDERS

The primary objective of the research described in this paper is to find a c^*-like quantity for flexible cylinders, which is capable of organizing response data for flexible cylinders. VIV on flexible cylinders tends to excite many modes. Furthermore they may be exposed to sheared flows and may possess spatially varying properties, such as the coverage of strakes and fairings. We seek an equivalent parameter, c^*_{eq}, which organizes response data in much the same way as the rigid cylinder data is organized in Figure 3.

In order to extend c^* to characterize the response of long flexible cylinders, new definitions are needed for response amplitude and system damping.

Figure 4 shows how the authors propose to model the damping of a long flexible cylinder in terms of an equivalent rigid cylinder. For a steady state response, the input power entering the long flexible cylinder must equal the output power dissipated by damping

$$\boldsymbol{\langle \Pi^{in} \rangle = \langle \Pi^{out} \rangle = \langle \Pi^{str} \rangle + \langle \Pi^{flux} \rangle} \quad (3)$$

Where $\langle \Pi^{in} \rangle$ is the time-averaged input power and $\langle \Pi^{out} \rangle$ is the time-averaged output power. The output power includes two terms, $\langle \Pi^{str} \rangle$ which is dissipated by the structural damping in the power-in region and $\langle \Pi^{flux} \rangle$, the power flux which leaves the power-in region and is dissipated by damping, both structural and hydrodynamic in the power-out region.

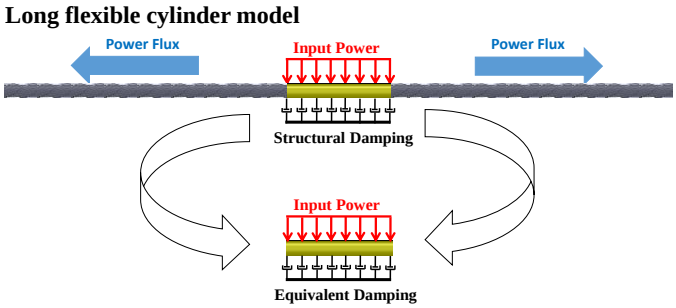

Figure 4 A conceptual model of the relationship between flexible cylinder damping and the damping of the equivalent rigid cylinder.

The basic principle to be applied is that the damper of the equivalent rigid cylinder must dissipate the same total power as that in the long flexible cylinder. The equivalent rigid cylinder has the length of the power-in region of the long flexible cylinder for each specific excitation frequency. For the data shown in this paper the power-in region is the bare region in the middle of the partially straked pipe, exposed to uniform flow. A key step is to find the damping coefficient, r_{eq}, of the equivalent damper from the experimental data.

In order to find c^*_{eq} and A^*_{eq}, three quantities must be evaluated, as shown in equations 4, 5 and 6.

The temporal root-mean-square (RMS) of the cross-flow displacement $y(z,t)$ at each location is defined as:

$$\boldsymbol{y_{rms}(z) = \sqrt{\frac{1}{T}\int_0^T y^2(z,t)dt}} \quad (4)$$

The spatial mean value of the temporal RMS displacement $y_{rms}(z)$ in the power-in region is defined as:

$$\boldsymbol{\mu = \frac{1}{L_{in}}\int_{L_{in}} y_{rms}(z)dz} \quad (5)$$

The spatial RMS of the temporal RMS displacement $y_{rms}(z)$ in the power-in region is defined as:

$$\boldsymbol{Y_{RMS}} = \sqrt{\frac{\mathbf{1}}{\boldsymbol{L_{in}}}\int_{L_{in}} \boldsymbol{y_{rms}^2(z)dz}} \quad (6)$$

The cylinder velocity is defined as:

$$\boldsymbol{\dot{y}_{rms}} = \boldsymbol{y_{rms}} * \boldsymbol{\omega} \quad (7)$$

Which is exact for a purely sinusoidal signal and approximately equal if $y(z,t)$ is a Gaussian narrow band signal, centered on the frequency ω.

- **Definition of the equivalent damping parameter c_{eq}^***

The basic idea of this energy conservation method is that the damping coefficient r_{eq} is defined so as to require the dissipated energy of the equivalent rigid cylinder be equal to that of the long flexible cylinder. The per unit length damping coefficient of the equivalent spring-mounted cylinder is defined as:

$$\boldsymbol{r_{eq}} = \frac{\langle \boldsymbol{\Pi^{out}} \rangle}{\int_{L_{in}} \frac{\mathbf{1}}{\boldsymbol{T}} \int_0^T \boldsymbol{\dot{y}^2(z,t)dzdt}} = \frac{\langle \boldsymbol{\Pi^{out}} \rangle}{\boldsymbol{L_{in} * \omega^2 Y_{RMS}^2}} \quad (8)$$

The calculation of $\langle \Pi^{out} \rangle$ is shown in Rao *et al.* (2014). z is the axial coordinate along the pipe. t is the time in seconds. T is the oscillation period of the pipe. The displacement $y(z,t)$ is a zero mean, narrow band random process, centered on the response frequency ω. $\dot{y}(z,t)$ is the velocity of the pipe. The damping coefficient r_{eq} has the units of *Ns/m*^{2}.

The equivalent damping parameter c_{eq}^* is then defined as:

$$\boldsymbol{c_{eq}^*} = \frac{\boldsymbol{2 r_{eq} \omega}}{\boldsymbol{\rho U^2}} \quad (9)$$

Similar to the definition of Vandiver's damping parameter, c_{eq}^* may be thought of as the c^* for an equivalent spring-mounted rigid cylinder of length L_{in}, and a constant damping coefficient per unit length of r_{eq}. The total damping for the equivalent spring-mounted cylinder is given by $R_{eq} = r_{eq} * L_{in}$.

- **Definition of the equivalent lift coefficient C_{Leq}**

The familiar model of VIV lift force per unit length is:

$$\boldsymbol{f(t)} = \boldsymbol{C_{Leq}} \frac{\mathbf{1}}{\mathbf{2}} \boldsymbol{D \rho U^2 sin(\omega t)} \quad (10)$$

Where C_{Leq} is the average lift coefficient in the power-in region. D is the hydrodynamic diameter of the pipe. ρ is the fluid density. U is the spatial RMS flow speed in the power-in region.

In this paper the goal is to find the equivalent C_{Leq} and equivalent c_{eq}^* from actual measured strain and acceleration data resulting from the displacement $y(z,t)$, which is a zero mean narrow band random process centered on the frequency ω. A model of the time dependence of the lift force is required which is formulated in terms of the measured velocity.

The following approximate formula is used to represent the time dependent part of Equation (10) when $y(z,t)$ is a narrow band signal:

$$\boldsymbol{g(t)} = \frac{\boldsymbol{\dot{y}(z,t)}}{\sqrt{\mathbf{2}} \boldsymbol{y_{rms} * \omega}} \quad (11)$$

It has the following properties:

(1) It is normalized to have a maximum value of 1.0.

(2) It requires the VIV lift force to be in phase with the cylinder velocity.

(3) It reduces to $sin(\omega t + \theta)$ when $y(z,t)$ is a simple harmonic function.

The equivalent lift coefficient C_{Leq} is assumed to be constant and generates the same power on the equivalent cylinder as that on the long flexible cylinder. The equivalent lift coefficient for the pipe under uniform flow is shown in Equation (12)

$$\boldsymbol{C_{Leq}} = \frac{\mathbf{1}}{\frac{\mathbf{1}}{\mathbf{2}}\boldsymbol{\rho U^2 D}} \frac{\langle \boldsymbol{\Pi^{in}} \rangle}{\int_{L_{in}} \frac{\mathbf{1}}{\boldsymbol{T}} \int_0^T \boldsymbol{g(t)\dot{y}(z,t)dzdt}} = \frac{\mathbf{1}}{\frac{\mathbf{1}}{\mathbf{2}}\boldsymbol{\rho U^2 D L_{in}}} \frac{\langle \boldsymbol{\Pi^{in}} \rangle}{\frac{\boldsymbol{\omega \mu}}{\sqrt{\mathbf{2}}}} \quad (12)$$

- **Relation between A_{eq}^*, c_{eq}^* and C_{Leq}**

Vandiver(2012) showed that $A^* = \frac{C_L}{c^*}$ by equating the input and output power on a rigid cylinder. In a similar manner we can equate the input and output power of our equivalent cylinder: $\langle \Pi^{in} \rangle = \langle \Pi^{out} \rangle$, we have

$$\boldsymbol{A_{eq}^*} = \frac{\boldsymbol{C_{Leq}}}{\boldsymbol{c_{eq}^*}} = \sqrt{\mathbf{2}} \frac{\boldsymbol{Y_{RMS}^2}}{\boldsymbol{\mu \cdot D}} \quad (13)$$

When the response is that of a rigid cylinder in uniform flows, Equation (13) reduces to A/D.

RESULTS

• Effect of power-in length on the equivalent amplitude A_{eq}^* at fixed Reynolds number

Figure 5 shows the equivalent amplitude A_{eq}^* versus the exposure length fraction L_{in}/L at a single Reynolds $Re = 60{,}000$. It is expected that the equivalent amplitude A_{eq}^* increases with the exposure length. The exposure length is the power-in length of the partially straked pipe in the uniform

flow. The longer the power-in region the greater the expected response.

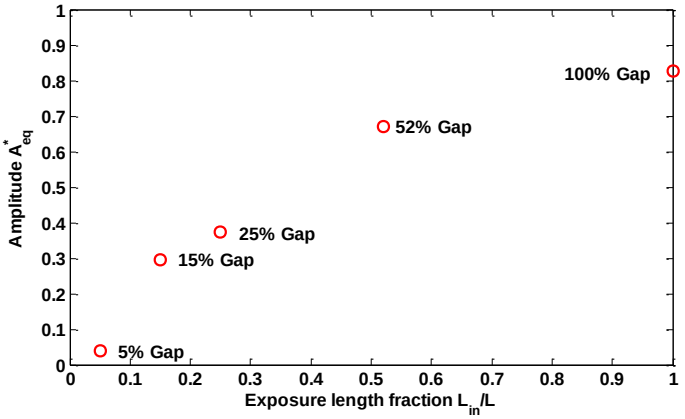

Figure 5 The equivalent amplitude A^*_{eq} versus the exposure length fraction L_{in}/L at $Re = 60{,}000 (m^* = 1.74)$ which corresponds to the flow speed of 0.75m/s.

Figure 6 shows the plot of the damping parameter c^*_{eq} versus the exposure length fraction L_{in}/L at $Re = 60{,}000$. The equivalent damping parameter c^*_{eq} includes contributions from both structural and hydrodynamic damping. In general, the contribution from the structure damping is very small compared to that from the hydrodynamic damping. Most of the hydrodynamic damping is represented by the energy flowing out of the power-in region as propagating waves. For long cylinders the equivalent total damping is constant due to the flow of energy away from the power-in region is approximately constant. Thus the equivalent damping parameter c^*_{eq} decreases as the exposure length increases. This effect is seen in Figure 6.

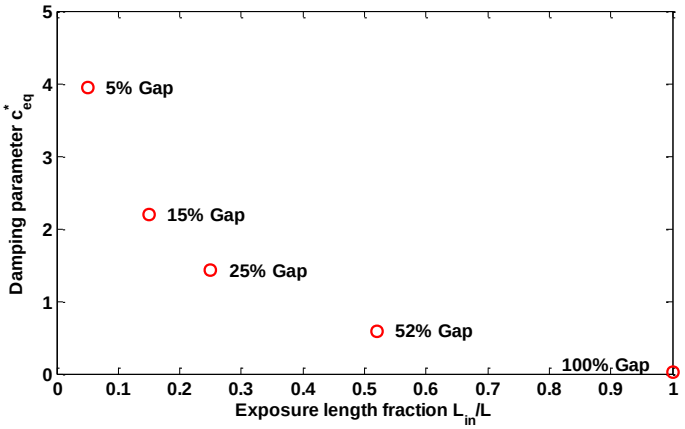

Figure 6 The equivalent damping parameter c^*_{eq} versus the exposure length fraction L_{in}/L at $Re = 60{,}000 (m^* = 1.74)$ which corresponds to the flow speed of 0.75m/s.

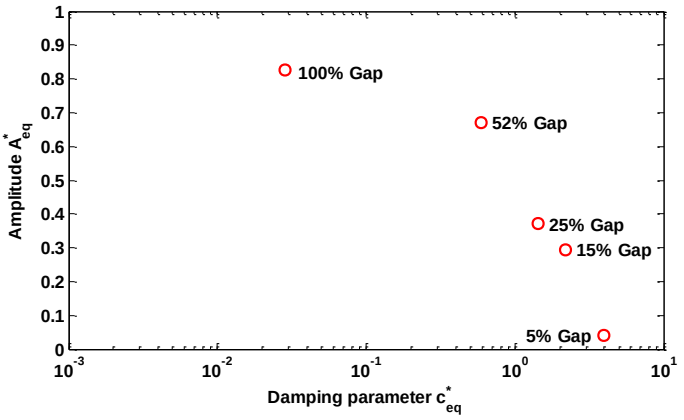

Figure 7 The equivalent amplitude A^*_{eq} versus the equivalent damping parameter c^*_{eq} at $Re = 60{,}000 (m^* = 1.74)$ which corresponds to the flow speed of 0.75m/s.

As shown in Fig.3, the peak amplitude A^*_{max} depends strongly on the Reynolds number. At a given Reynolds number, peak amplitude A^*_{max} collapses to a single curve when plotted versus c^*.

Figure 7 shows the equivalent amplitude A^*_{eq} versus the equivalent damping parameter c^*_{eq} at the Reynolds number $Re = 60{,}000$. The same trend of amplitude decreasing as damping increases that was visible in Figure 3 is also seen in Figure 7. The maximum equivalent amplitude A^*_{eq} occurs at the minimum equivalent damping parameter c^*_{eq} which corresponds to the bare pipe case. For the bare pipe, the whole region is considered as the power-in region and only structural damping exists. Thus the bare pipe tends to have the smallest possible equivalent damping parameter.

• Effect of Reynolds number on the equivalent amplitude A^*_{eq}

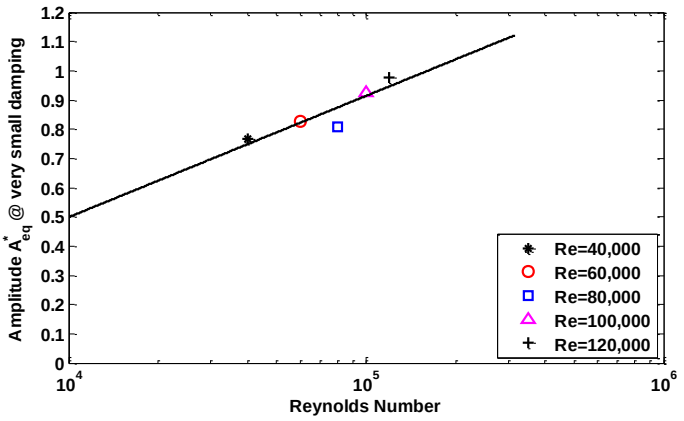

Figure 8 The equivalent amplitude A^*_{eq} at very low equivalent damping parameter from $D = 80mm$ bare pipe, showing a

linear increase in A^*_{eq} versus the log of the Reynolds.

In order to investigate the effect of Reynolds number on response amplitude, a number of cases at the same damping parameter should be chosen. Govardhan and Williamson (2006) chose the zero damping case to extract the effect of Re on A^*. The minimum damping cases for the Shell experiments were those with 100% exposure in a uniform flow. In these cases only structural damping acted on the cylinder. The response was quite large and is on the response plateau which maxes out at the A^* corresponding to a lift coefficient of zero. The measured damping was approximately 0.6% in air. The response at this minimum level of damping is used here to approximate the zero damping case.

A bare pipe with 80mm diameter at five different Reynolds number was chosen to investigate the effect of Reynolds number on the amplitude.

Figure 8 shows the plot of the equivalent amplitude A^*_{eq} versus Reynolds number. The equivalent amplitude A^*_{eq} varies linearly with $log(Re)$ over the range of Reynolds numbers tested. It is not expected to remain linear outside of the range tested. A least-squares fit of all the data in Figure 8 suggests the best-fit curve is given by:

$$\boldsymbol{A^*_{eq}\big|_{@c^*_{eq}=0} = f(Re) = log(0.07 \times Re^{0.42})} \qquad (14)$$

This result is assumed to be the same as would be seen in a true zero damping case. We will use it to plot $A^*_{eq}/f(Re)$

- **Modified equivalent amplitude $A^*_{eq}/f(Re)$ versus equivalent damping parameter c^*_{eq}**

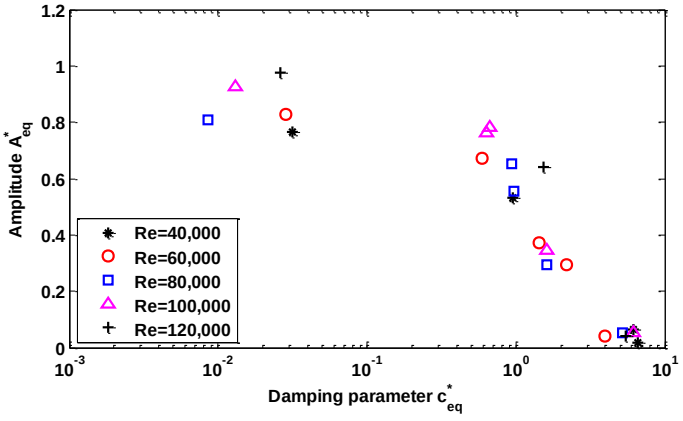

Figure 9 The equivalent amplitude A^*_{eq} versus the equivalent damping parameter c^*_{eq} for five partially straked pipes at five different Reynolds numbers.

Figure 9 shows A^*_{eq} versus c^*_{eq} before accounting for Reynolds number. The data has a considerable amount of scatter.

The modified equivalent amplitude $A^*_{eq}/f(Re)$ is the equivalent amplitude A^*_{eq} after removing the effect of Reynolds number

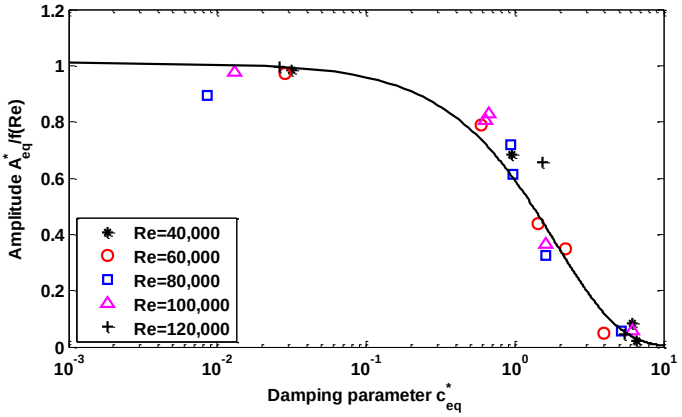

Figure 10 The modified amplitude $A^*_{eq}/f(Re)$ versus the equivalent damping parameter c^*_{eq} for five partially straked pipes at five different Reynolds numbers, all of the data collapses well onto a single curve.

Govardhan and Williamson (2006) mentioned that the effect of Reynolds number and the effect of mass-damping on the peak response could be separated. For bare pipes in uniform flows, the equivalent damping parameter is very small and has a very small effect on the equivalent amplitude. The only main factor to affect the equivalent amplitude will be Reynolds number. Thus the best-fit for Reynolds number has already been obtained through the equivalent amplitude at very small equivalent damping. The best-fit curve in Equation (14) is also applicable to the equivalent amplitude at large equivalent damping case, such as the pipe partially covered with helical strakes in uniform flow.

Figure 10 shows the equivalent amplitude after removing the effect of Reynolds number at both small and large damping parameters. All of the data collapses well onto a single curve. A good representation of this curve is given by Equation (15).

$$\boldsymbol{A^*_{eq}/f(Re) = e^{-0.534 \times c^*_{eq}}} \qquad (15)$$

Govardhan and Williamson (2006) applied a simple quadratic function to best fit the modified peak amplitude, see Equation (2). However, such a quadratic relationship cannot represent the response well for very low modified peak amplitude of order ~0.1 found at much larger damping parameter. Here, an exponential function is used to best fit the modified amplitude $A^*_{eq}/f(Re)$ based on two reasons. Firstly, the exponential form captures well the physics of VIV. At a much larger damping parameter, the modified amplitude $A^*_{eq}/f(Re)$ tends to be zero. A good example will be a pipe with 100% helical strake coverage in a uniform flow. This case is considered as almost zero amplitude but much larger damping.

Another reason is that this exponential form is much simpler but has a comparable performance to the quadratic function even in the small damping region (Govardhan and Williamson, 2006). It should be noted that not all of these data in Fig.10 are exactly on the best-fit curve. The possible explanation will be the effect of reduced velocity. Govardhan and Williamson (2006) investigated the peak response versus the Reynolds number and mass-damping but at one reduced velocity ~5.9. In Fig.10, the reduced velocity is not fixed at one value but varies from test to test.

CONCLUSIONS

A method is proposed to model the long flexible cylinder as an equivalent rigid cylinder. It shows that the use of the damping parameter c^* may be extended to the long flexible cylinder. SHELL Exploration and Production Company conducted a systemic VIV experiments for 80mm diameter pipe equipped with helical strakes in uniform flow, which enabled the investigation of damping on a long flexible cylinder.

It was demonstrated that the equivalent amplitudes depend not only on the equivalent damping but also on Reynolds number. By changing the coverage of helical strakes and thus changing the hydrodynamic damping, it was possible to examine the dependence of the equivalent amplitude on the equivalent damping parameter at a constant Reynolds number. It was demonstrated that the equivalent amplitude and the equivalent damping parameter follows a single curve. The dependence of equivalent amplitudes on Reynolds number could be obtained by investigating the bare pipe without helical strakes (which have very little damping) at different Reynolds numbers. It shows that the equivalent amplitude linearly increases with the log of the Reynolds number. If one accounts for Reynolds number, all of the data from long flexible cylinders in the SHELL Test collapse onto a single curve.

Extending this analysis to flexible pipes in sheared currents is more challenging and is still a topic of research.

ACKNOWLEDGMENTS

The authors gratefully acknowledge Deepstar and the SHEAR7 JIP members (AMOG Consulting, BP, Chevron, ConocoPhillips, ExxonMobil, Petrobras, SBM, Shell, Statoil & Technip) for supporting this research, and especially SHELL Exploration and Production for providing the data. We also thank Dr.Themistocles L.Resvanis for valuable discussions.

REFERENCES

Govardhan, R.N., Williamson, C.H.K., 2006. Defining the 'modified griffin plot' in vortex-induced vibration: revealing the effect of Reynolds number using controlled damping. Journal of Fluid Mechanics 561, 147-180.

Griffin, O.M., Skop, R.A., Ramberg, S.E., 1975. The Resonant, Vortex-Excited Vibrations of Structures and Cable Systems, Proceedings of the 1975 Offshore Technology Conference, Houston, Texas, May 5-8, 731-744.

Klamo, J.T., Leonard, A., Roshko, A., 2005. On the maximum amplitude for a freely vibrating cylinder in cross-flow. Journal of Fluids and Structures 21, 429-434.

Lie, H., Braaten, H., Jhingran,V., Sequeiros, O.E., Vandiver, J.K., 2012, Comprehensive Riser VIV Model Tests in Uniform and Sheared Flow, Paper OMAE2012-84055, Proc. of OMAE Conference, Rio de Janeiro, Brazil.

MARINTEK, 2011. Shell Riser VIV Tests Main Report, No. 580233.00.0

Rao, Z., 2015. The flow of power in the vortex-induced vibration of flexible cylinders. PhD diss., Massachusetts Institute of Technology.

Rao, Z., Resvanis, T.L. and Vandiver, J.K., 2014, The identification of power-in region in vortex-induced vibration of flexible cylinders, Paper OMAE2014-24472, Proc. of OMAE Conference, San Francisco, CA, USA

Rao, Z., Vandiver, J.K. and Jhingran, V., 2013, VIV excitation competition between bare and buoyant segments of flexible cylinders, Paper OMAE2013-11296, Proc. of OMAE Conference, Nantes, France.

Rao, Z., Vandiver, J. K., & Jhingran, V., 2015, Vortex induced vibration excitation competition between bare and buoyant segments of flexible cylinders. *Ocean Engineering*, *94*, 186-198.

Rao, Z., Vandiver, J.K., Jhingran, V. and Sequeiros, O., 2012. The Effect of Exposure Length on Vortex induced vibration of flexible cylinders, Paper OMAE2012-83273, Proc. of OMAE Conference, Rio de Janeiro, Brazil.

Resvanis, T.L., Jhingran, V., Vandiver, J.K., Liapis,S., 2012. Reynolds Number Effects on the Vortex-Induced Vibration of Flexible Marine Risers, Paper OMAE2012-83565, Proc. of OMAE Conference, Rio de Janeiro, Brazil.

Resvanis, T.L., Rao, Z. and Vandiver, J.K., 2014. Effects of Strake Coverage and Marine Growth on Flexible Cylinder VIV, Paper OMAE2014-24462, Proc. of OMAE Conference, San Francisco, CA, USA

Sarpkaya, T. 2004, A critical review of the intrinsic nature of vortex-induced vibrations, Journal of Fluids and Structures 19, No 4, 389-447.

Scruton, C., 1965. On the Wind-Excited Oscillations of Stacks, Towers, and Masts, In: Conference Proceedings of 1963 National Physical Laboratory, Teddington, UK.

Vandiver, J.K., 2012. Damping parameters for flow-induced vibration, Journal of Fluids and Structures 35, pp.105-119.